Journal of Asian Ceramic Societies

ISSN: (Print) 2187-0764 (Online) Journal homepage: https://www.tandfonline.com/loi/tace20

Structural and chemical analysis of silica-doped β-TCP ceramic coatings on surgical grade 316L SS for possible biomedical application

Karuppasamy Prem Ananth, Sudha Shanmugam, Sujin P. Jose, A. Joseph Nathanael, Tae Hwan Oh, Devanesan Mangalaraj & Anbalagan M. Ballamurugan

To cite this article: Karuppasamy Prem Ananth, Sudha Shanmugam, Sujin P. Jose, A. Joseph Nathanael, Tae Hwan Oh, Devanesan Mangalaraj & Anbalagan M. Ballamurugan (2015) Structural and chemical analysis of silica-doped β-TCP ceramic coatings on surgical grade 316L SS for possible biomedical application, Journal of Asian Ceramic Societies, 3:3, 317-324, DOI: 10.1016/j.jascer.2015.06.004

To link to this article: https://doi.org/10.1016/j.jascer.2015.06.004

Journal of Asian Ceramic Societies 3 (2015) 317–324

HOSTED BY

Contents lists available at ScienceDirect

Journal of Asian Ceramic Societies

journal homepage: www.elsevier.com/locate/jascer

Structural and chemical analysis of silica-doped β-TCP ceramic coatings on surgical grade 316L SS for possible biomedical application

Karuppasamy Prem Ananth [a,*], Sudha Shanmugam [a], Sujin P. Jose [b,1], A. Joseph Nathanael [c], Tae Hwan Oh [c], Devanesan Mangalaraj [a], Anbalagan M. Ballamurugan [a,**]

[a] Department of Nanoscience and Technology, Bharathiar University, Coimbatore 641046, India
[b] Department of Materials Science and Nanoengineering, Rice University, Texas 77005, USA
[c] Department of Nano, Medical and Polymer Materials, Yeungnam University, Gyeongsan 712-749, South Korea

ARTICLE INFO

Article history:
Received 27 April 2015
Received in revised form 15 June 2015
Accepted 19 June 2015
Available online 8 July 2015

Keywords:
β-Tricalcium phosphate
Silica
Biomineralization
Electrophoretic deposition

ABSTRACT

We have developed a novel approach to introduce silica-doped β-tricalcium phosphate (Si-β-TCP) on 316L SS substrates for enhanced biological properties. Doping of β-TCP with silica loadings ranging from 0 to 8 mol% was carried out using chemical precipitation method. Si-β-TCP powder was sintered at 800 °C followed by coating it on 316L SS substrate using electrophoretic deposition. The coated and uncoated samples were investigated by various characterization techniques such as X-ray diffraction (XRD), Fourier transform infrared spectroscopy (FTIR), field emission scanning electron microscopy (FESEM) and X-ray fluorescence spectroscopy (XRF). Biomineralization ability of the coatings was evaluated by immersing in simulated body fluid (SBF) solution for different number of days such as 7, 14, 21 and 28 days. The results obtained in our study have shown that the apatite formation ability was high for the 8 mol% of Si-β-TCP. This will promote better biomineralization ability compared to the other coatings.

1. Introduction

The appropriate bioactive, biocompatible, stronger and inexpensive synthetic materials are essential for biomedical application. Hydroxyapatite (HAp) and β-tricalcium phosphate (β-TCP) are extensively used as potential bioceramics for both dental and orthopedic applications due to their close chemical similarity with the inorganic component of bone and tooth mineral [1]. HAp has received more attention as bone replacing materials in orthopedic surgery because of its inherent ability to bond with the hard tissue [2]. But it has a low resorption rate and bone growth occurs only at the interface [3]. The stoichiometric synthetic HAp does not degrade completely and remnants of this are found after a long period of the implantation [4]. But β-TCP exhibits optimal level of solubility in biological fluid and the chemical composition is similar to apatite present in bone tissues. Hence, this material has extensively been used for bone grafting [5]. β-TCP is an attractive biomedical material owing to its excellent biocompatibility and the nontoxicity of its chemical components. It also serves as a potential precursor for Ca and PO_4^{3-} ions and allows new bone formation [6].

In this regard, β-TCP has an upper hand that it is a potential resorbable bioceramic, and has good dissolution rate control than stoichiometric HAp [7]. But it contributes a threat to the reduction in implant strength and its dissolution rate is altered by chemical modification. The crystallographic study of β-TCP revealed that the Ca (4) and Ca (5) are distinct from the other three sites and are ideal for substitution with smaller cations. Ca (4) having coordination number of 3 in the flattened tetrahedral configuration has an unusual coordination to O (9), O (9′) and O (9″) face of P (1) O_4 group resulting in compressed Ca site. Ca (4)···O (9) bond length is 3.041 Å and longer than the normal Ca···O bonds of length 2.4 Å. Ca (5) sites are surrounded by O in sixfold distorted octahedral coordination, thus making small ionic substitution possible [8,9].

TCP exhibits three polymorphs and they are β-TCP, stable below 1180–1400 °C, α-TCP, stable in the temperature range 1180–1400 °C and α′-TCP, observed above 1470 °C [10,11]. Ionic inclusions are done in order to stabilize the β-TCP structure. PO_4^{3-} and SiO_4^{4-} have similar tetrahedral structure. This feature could

* Corresponding author. Tel.: +91 422 2425458.
** Corresponding author. Tel.: +91 422 2428421.
E-mail addresses: kpananth01@gmail.com (K. Prem Ananth), balamurugan@buc.edu.in (A.M. Ballamurugan).
[1] Address: School of Physics, Madurai Kamaraj University, Madurai 625021, India.
Peer review under responsibility of The Ceramic Society of Japan and the Korean Ceramic Society.

http://dx.doi.org/10.1016/j.jascer.2015.06.004

be exploited to replace P by Si. Recently numerous studies have specified that Si-based materials can play a vital role in bone formation [12]. Silica has a unique relationship with calcium because it works to attract calcium to bone. Bone calcification helps to form new bone and strengthens mature bone [13]. The silica substituted calcium phosphate demonstrated osteoinductive properties and significantly increased the amount of bone that formed compared to the calcium phosphate implants [14]. Different coating technologies like biomimetic, pulsed laser deposition, electrochemical deposition, plasma spraying, electrophoretic, micro-arc method, etc. [15–20] have been adopted for the development of Si-β-TCP coating on the implant. Among the several coating methods, electrophoretic deposition (EPD) operates with mild conditions and forms crystalline deposits with low residual stresses and thus it becomes a promising method for preparing coatings on surgical grade implants [21].

The impact of this investigation is to find a better way to prepare novel bioactive and biocompatible materials for orthopedic implants. In this study, we have mainly focused on Si-β-TCP bioceramic coating on 316L SS using electrophoretic deposition and characterized it by various techniques in order to enhance the biomineralization activity. These materials exhibit improved biomineralization in SBF solution. This study would be beneficial not only for the academic or scientific community but also for the general public due to the widespread application in healthcare. Further, this work will provide necessary information to the future researchers on the recent status of the biomaterials, and issues of bioimplants and on enhancing the properties. The effects of crystallinity, functional group, size and morphology of 0, 2, 4, 5 and 8 mol% of Si-β-TCP are explained in detail (the code numbers are mentioned as 0Si-β-TCP, 2Si-β-TCP, 4Si-β-TCP, 5Si-β-TCP and 8Si-β-TCP respectively for 0, 2, 4, 5 and 8 mol% Si-doped β-TCP). To the best of our knowledge, no reports are available on Si-β-TCP coating on 316L SS. In a nut shell, this new coating material Si-β-TCP will be a promising candidate for high load-bearing orthopedic implants such as hip, knee and shoulder joints.

2. Materials and methods

2.1. Materials

Calcium nitrate tetrahydrate ($Ca(NO_3)_2{\cdot}4H_2O$, Himedia) and diammonium hydrogen phosphate ($(NH_4)_2HPO_4$, Himedia) were used as precursors for calcium (Ca) and phosphate (P) respectively. Ammonium hydroxide (NH_4OH) was used to maintain the pH and tetraethylorthosilicate Si ($OCH_2CH_3)_4$ (TEOS) was used as a silica (Si) precursor. All the chemicals used were of analytical grade. Deionized water was used in all synthesis steps.

2.2. Synthesis of β-TCP bioceramic powders

2 M of Ca $(NO_3)_2{\cdot}4H_2O$ and 1.33 M of $(NH_4)_2HPO_4$ were dissolved in 200 ml of deionized water separately and stirred vigorously. $(NH_4)_2HPO_4$ solution was added drop wise to vigorously stirred Ca $(NO_3)_2{\cdot}4H_2O$ solution at room temperature to obtain a milky solution. The Ca/P molar ratio of initial reagents was 1.5. The pH of the final solution was adjusted to 8.5 by adding NH_4OH solution. The milky white precipitate thus obtained was stirred for 1 h and solution was then filtered and washed with water to remove any excess NH_4OH. The filtered cake was dried in an oven at 120 °C overnight. The as-dried powders were crushed and sintered at 800 °C for 2 h.

2.3. Synthesis of Si-β-TCP bioceramic powders

The synthesis of four different Si-β-TCP compositions was carried out as follows; Stoichiometric pure β-TCP and four different 2Si-β-TCP, 4Si-β-TCP, 5Si-β-TCP and 8Si-β-TCP were prepared by chemical precipitation method using $Ca(NO_3)_2{\cdot}4H_2O$, $(NH_4)_2HPO_4$ and $Si(OCH_2CH_3)_4$ (TEOS) as precursors. The starting materials with a Ca/(P + Si) ratio of 1.5 were mixed and different mol% of TEOS like 0, 2, 4, 5 and 8 were added to calcium nitrate tetrahydrate aqueous solution under stirring along with drop wise addition of the diammonium hydrogen phosphate. The pH of the suspension was maintained at 8.5 by adding required amounts of NH_4OH solution. After the required pH is reached, the solution was washed with water to remove any excess NH_4OH. The precipitate was dried in an oven at 120 °C overnight and the as-dried sample was crushed and sintered at 800 °C for 2 h in a muffle furnace.

Table 1
Ion concentrations (mmol/dm^3) of SBF and human blood plasma.

Ionic concentration (mmol/dm^3)	Simulated body fluid	Blood plasma
Na^+	142	142
K^+	5.0	5.0
Mg^+	1.5	1.5
Ca^+	2.5	2.5
Cl^-	147.8	103.0
HCo^{3-}	4.2	27.0
HPO^{4-}	1.0	1.0
So^{4-}	0.5	0.5

2.4. Substrate preparation

The 316L SS specimens used in the present study were cut into 10 mm × 10 mm × 2 mm dimensions. Prior to the study, the metal specimens were mechanically polished using silicon carbide papers of 80–800 grit size. Final polishing was done using fine (0.3–0.4 μm) diamond paste in order to obtain scratch-free mirror finish surface. The polished specimens were washed with distilled water and then ultrasonically degreased with acetone [22].

2.5. Preparation of Si-β-TCP substrate

The synthesized pure β-TCP and Si-β-TCP powders were used as coating materials for deposition on 316L SS substrate by EPD technique. 2.5 g of β-TCP powders were mixed with 60 ml isopropanol using a magnetic stirrer for obtaining a homogeneous colloidal suspension. The substrate alloy (working electrode) and the platinum counter electrode were immersed in the suspension. The distance between the two electrodes was 1 cm. The deposition was carried out at various potentials by trial and error method and the deposition condition was optimized. The optimized potential and current were 103 V and 400 mA for 3 min. The coated substrate were dried at room temperature and heat treated at 400 °C for 2 h. The same procedure was adopted for the coating of 2Si-β-TCP, 4Si-β-TCP, 5Si-β-TCP and 8Si-β-TCP.

2.6. Biomineralization ability in SBF

The evaluation of biomineralization ability was carried out in Kokubo's simulated body fluid (SBF) [23], the composition of which is presented in Table 1. The solution was kept at 37 °C, and the pH was regulated to be in the range of 7.3–7.4. The biomineralization test was carried out by soaking the coated samples mounted vertically in a special platinum holder in 45 ml of SBF in polyethylene containers maintained at 37 °C for various time periods (7, 14, 21 and 28 days). After that the samples were gently rinsed with deionized water to remove SBF solutions followed by drying at room temperature.

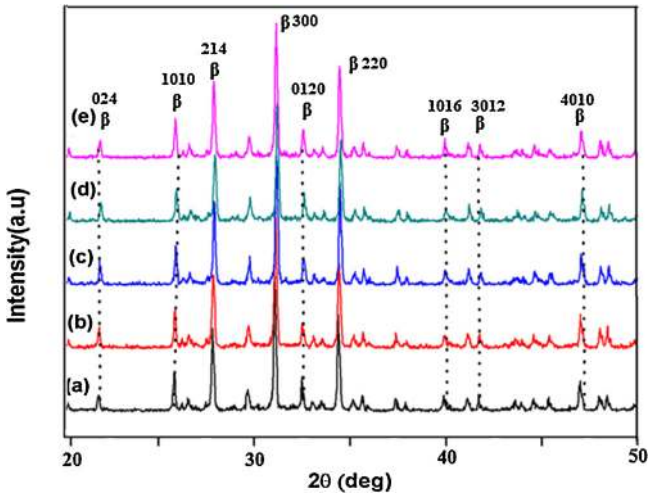

Fig. 1. XRD pattern of (a) 0Si-β-TCP, (b) 2Si-β-TCP, (c) 4Si-β-TCP, (d) 5Si-β-TCP and (e) 8Si-β-TCP.

2.7. Characterization

The structural analysis of pure β-TCP and Si-β-TCP particles was carried out on a Philips PW 1730 X-ray diffractometer using Cu Kα radiation at 35 kV and 30 mA at room temperature. The XRD data were collected over 2θ range 20–60° at a step size of 0.02°/s. Fourier transform infrared spectroscopy (FTIR) (Thermo Nicolet Model: 6700) was used to study the functional groups in the wavenumber range of 4000–400 cm^{-1}. The samples were investigated for their microstructural and morphological features by a scanning electron microscope (SEM) (Hitachi, Model: S-3400 N) and a field emission scanning electron microscope (FEG, quanta 250, FEI company) that was operated by a typical accelerating voltage of 20 kV and equipped with an energy-dispersive X-ray spectroscopy (EDXS) analyzer. Prior to SEM examination, all the samples were sputter-coated by carbon to minimize any possible surface charging effects. The quantitative chemical analysis of Ca, P and Si in pure β-TCP and Si-β-TCP nanoparticles was determined by wavelength dispersive X-ray fluorescence spectrometer (WD-XRF) (Bruker, Model: S4 Pioneer) provided with an Rh X-ray tube and a power generator of 2.4 kW. Powdered samples weighing 2.5 g were mixed with boric acid and melted in an alumina crucible and disks were formed in a special controlled furnace.

3. Results and discussion

3.1. X-ray diffraction powder

Fig. 1 shows the XRD pattern of β-TCP and Si-β-TCP powders sintered at 800 °C. The sintered temperature plays an important role in the formation of β-TCP. The presence of all sharp peaks in the spectrum confirms the formation of β-TCP with high crystallinity and small crystallite size. The crystallite sizes were calculated using Debye Scherrer's formula. $D = 0.9\lambda/\beta\cos\theta$, where λ is the wavelength of Cu Kα radiation and β is the FWHM value. The majority of the diffraction peaks at 2θ values of 21.9°, 25.8°, 27.8°, 29.7°, 31.1°, 34.4°, 39.8°, 41.7° and 48° are assigned to corresponding $h\,k\,l$ value planes (0 2 4), (1 0 1 0), (2 1 4), (3 0 0), (0 2 1 0), (2 2 0), (1 0 1 6), (3 0 1 2) and (4 0 1 0) respectively for β-TCP phase in rhombohedral structure (space group R3c, $Z = 21$) with the unit cell parameters $a = b = 10.3958(1)$ Å, $c = 37.3122(7)$ Å, $\alpha = \beta = 90°$ and $y = 120°$ in the hexagonal setting. This is in good agreement with the standard JCPDS card no. (09-0169). The intensity of the peak corresponding to the plane (0 2 1 0) increases indicating the deficiency of calcium

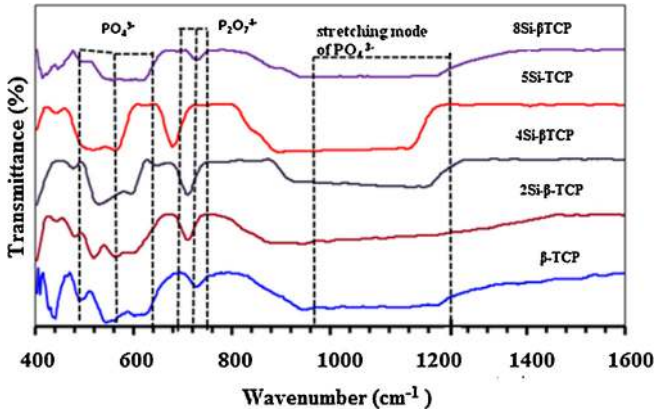

Fig. 2. FTIR spectra of pure β-TCP, 2Si-β-TCP, 4Si-β-TCP, 5Si-β-TCP and 8Si-β-TCP.

in β-TCP. It can be seen that the samples fabricated from sintered (at 800 °C) powder are highly crystalline and consist of single-phase β-TCP [24]. The average crystallite size of the pure β-TCP is found to be 76.54 nm. The XRD pattern of all the samples appeared to be identical indicating the incorporation of Si into the β-TCP lattice had no direct effect on its crystallographic structure with an exception of some intensity changes. These variations are very small and presumably due to the partial Si incorporation. This may be due to the formation of a crystalline or amorphous silicate, as a separate phase. Table S1† shows the XRD patterns of pure β-TCP and Si-β-TCP powders. Pure β-TCP exhibited higher grain size of 76.54 nm in comparison with the Si-β-TCP samples. With the increase in Si (0–8 mol%) content, there is a gradual decrease in grain size (76.54, 75. 95, 74.04, 70.56 and 66.28 nm) for 0Si-β-TCP, 2Si-β-TCP, 4Si-β-TCP, 5Si-β-TCP and 8Si-β-TCP respectively.

3.2. Fourier transform infrared spectroscopy

Fourier transform infrared (FTIR) spectroscopy was used to determine the functional group of the synthesized pure β-TCP and Si-β-TCP powders. The spectra of the as-prepared β-TCP and Si-β-TCP powders sintered at 800 °C are shown in Fig. 2. The bands over the range 1222.6–946.9 cm^{-1} represent the stretching mode of PO_4^{3-} group. The sharp peaks from 617.1 to 547.7 cm^{-1} represent the symmetric vibration of PO_4^{3-} indicating the presence

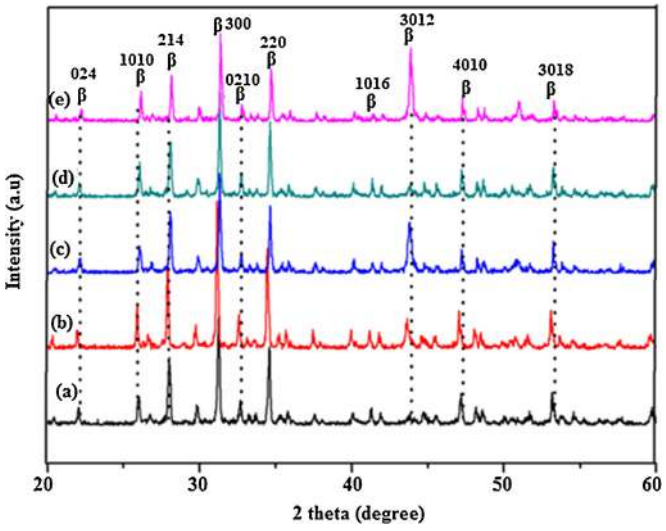

Fig. 3. XRD pattern of (a) 0Si-β-TCP, (b) 2Si-β-TCP, (c) 4Si-β-TCP, (d) 5Si-β-TCP and (e) 8Si-β-TCP coatings on surgical grade 316L SS.

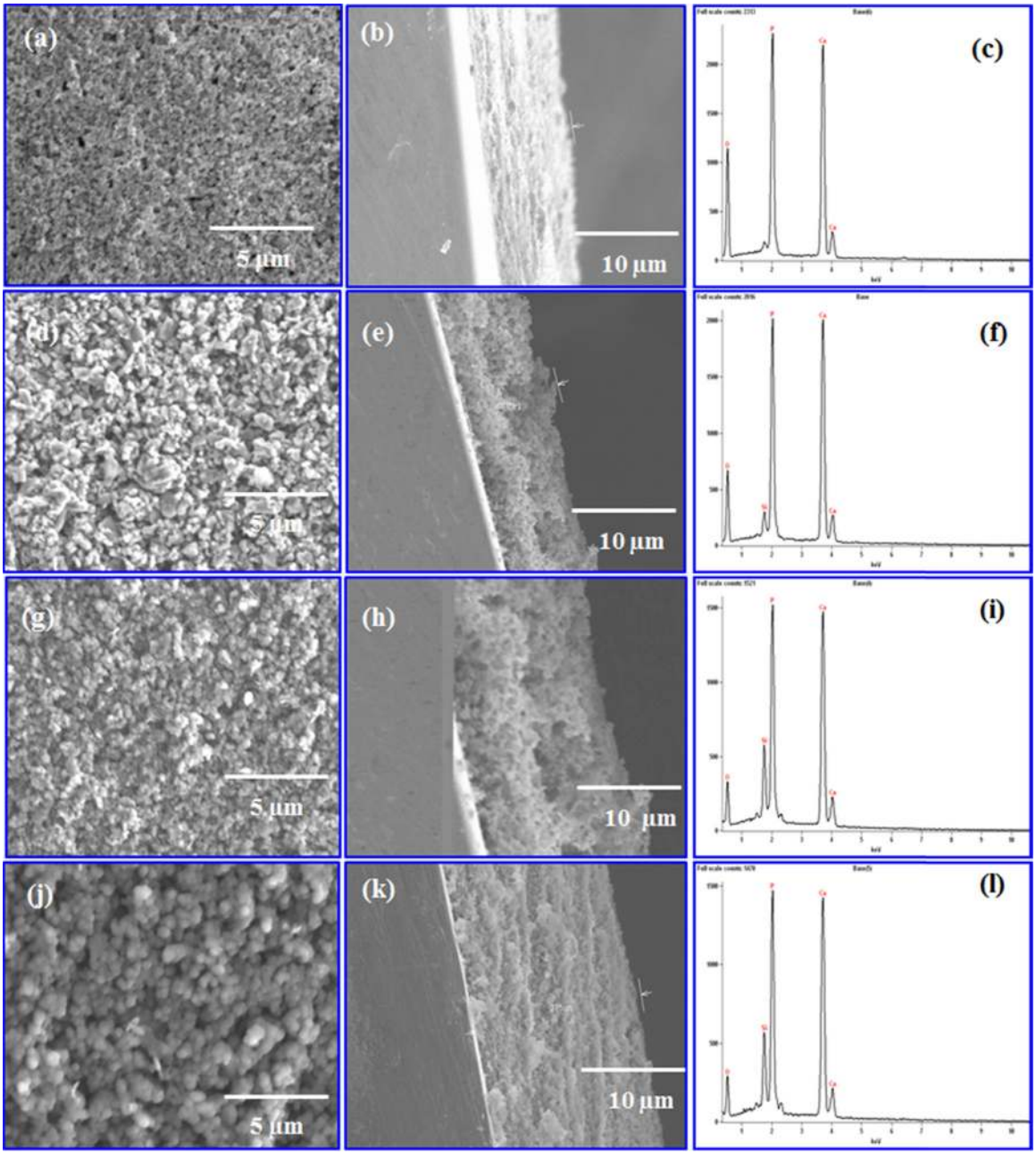

Fig. 4. SEM morphology, cross-sectional view and EDX analysis of (a–c) pure β-TCP, (d–f) 2Si-β-TCP, (g–i) 4Si-β-TCP and (j–l) 8Si-β-TCP coated 316L SS substrate.

of β-TCP phases [25]. When compared to pure β-TCP and Si-β-TCP, pronounced intensity variation is observed for pure Si-β-TCP [26]. The FTIR spectrum of all Si-β-TCP samples shows the vibration modes of PO_4^{3-} ions in the range of 500–600 (503.3, 570.8, 550, 582.4), 1200–950, and 650 cm^{-1}. The bending of hydroxyl group (OH) is assigned to 617.1 cm^{-1}. Disappearance of OH bending is observed as the molar ratio of Si is increased and this may be due to the transformation of calcium deficient apatite to β-TCP. The bands obtained at 727 cm^{-1} and 946 cm^{-1} are ascribed to the symmetric and asymmetric bridge P—O stretching modes. The bands obtained at 613, 567, 540, 527 and 455 cm^{-1} are certainly due to the asymmetric bending vibrations of terminal P—O bonds. The symmetric bending vibrations of P—O bonds are assigned to 582.4 cm^{-1}. The peaks in the region of 727–730 cm^{-1} could be attributed to the presence of pyrophosphate groups ($P_2O_7^{4-}$). There is little evidence of a shift in the position of these peaks with silica content, but the trend observed in the infrared data for the bands associated with PO_4^{3-} are consistent with a change in the dominant crystal structure from β-TCP. Moreover, the spectra for all the Si-β-TCP samples confirm the existence of silicon. These results also show that PO_4^{3-} tetrahedrons are replaced by SiO_4^{4-} tetrahedrons in the β-TCP structure. However slight peak broadening indication are observed, that could identify the substitution of P by Si.

3.3. X-ray diffraction coating

Fig. 3 shows the XRD pattern of the pure β-TCP and Si-β-TCP coatings on 316L SS treated at a temperature of 400 °C for 2 h. The majority peaks observed in all the samples of β-TCP suggest that no thermal decomposition has occurred at 400 °C. By comparing XRD patterns of Si-β-TCP and pure β-TCP coatings on 316L SS, it is observed that there are slight changes in the intensity of the

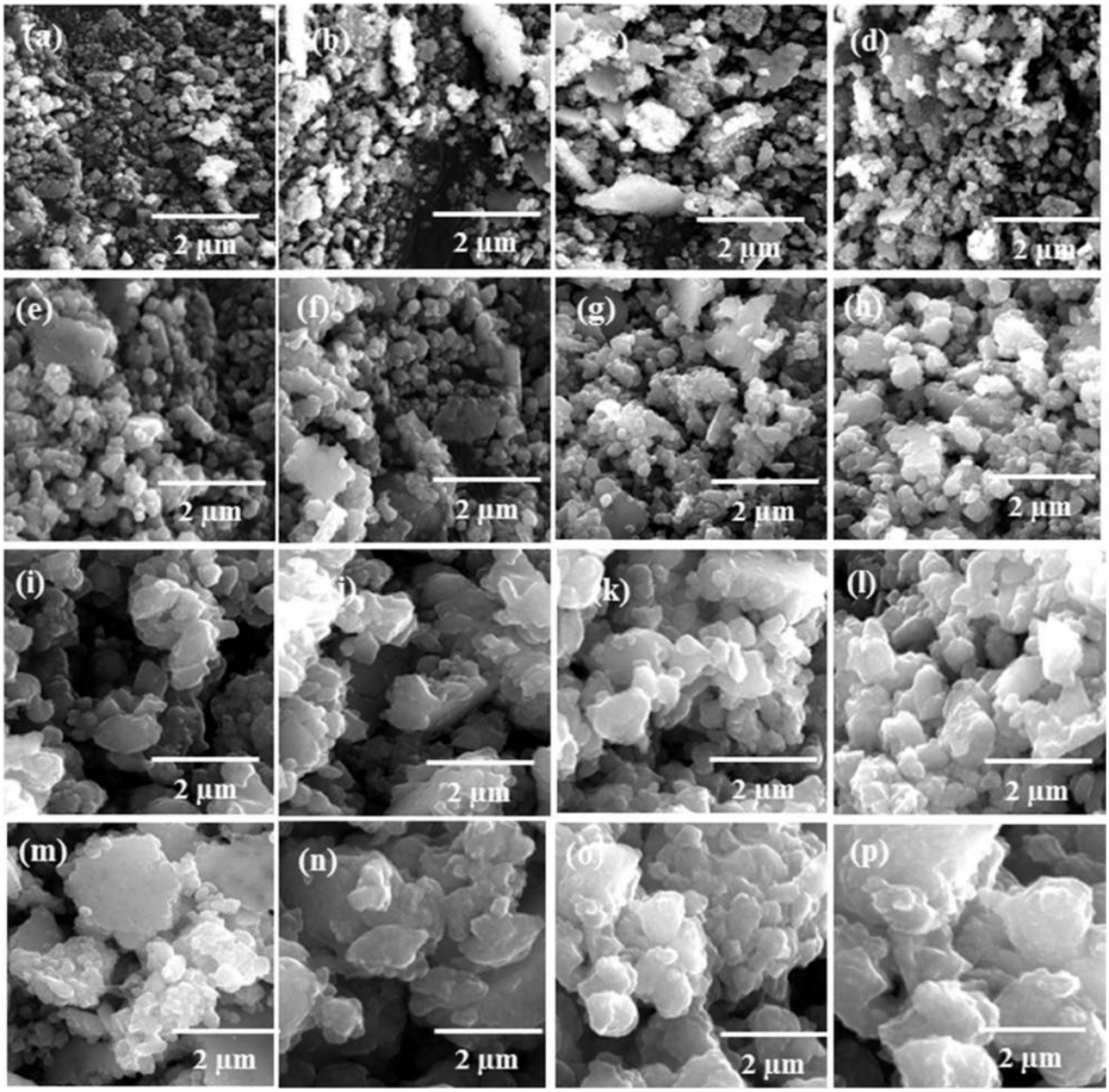

Fig. 5. FE-SEM morphology of (a–d) pure β-TCP, (e–h) 2Si-β-TCP, (i–l) 4Si-β-TCP and (m–p) 8Si-β-TCP coating on 316L SS substrate soaked in SBF solution for 7, 14, 21 and 28 days – in vitro bioactivity analysis.

peaks position. The majority of the diffraction peaks at 2θ values of 22.1°, 25.1°, 28.0°, 31.2°, 34.6°, 47.2° and 53.2° are assigned to corresponding *h k l* value planes (0 2 4), (1 0 1 0), (2 1 4), (3 0 0), (2 2 0), (4 0 1 0) and (3 0 1 8) of β-TCP coatings on 316L SS. This is in good agreement with the standard JCPDS card no. (09-0169) rhombohedral structure. The XRD pattern confirms the formation of pure β-TCP and Si-β-TCP phases and no other extra peaks are detected in this pattern. Table. S2† shows the crystallite sizes estimated for pure and Si-β-TCP having different concentrations coated on 316L SS. The average crystallite size for pure β-TCP coating is calculated using Debye Scherrer's formula as 88.72 nm. The increase in the percentage of silica in β-TCP brings a corresponding decrease in crystallite size (86.8, 72.7. 66.8, and 66.2 nm respectively for 2Si-β-TCP, 4Si-β-TCP, 5Si-β-TCP and 8Si-β-TCP). All the Si-β-TCP coatings retained the rhombohedral structure and no appreciable difference is observed in the XRD patterns of the coated substrate.

3.4. SEM image of pure β-TCP and Si-β-TCP

Fig. 4a–i shows the surface morphology, cross-sectional view and EDX analysis of the pure β-TCP, 2Si-β-TCP, 4Si-β-TCP and 8Si-β-TCP coated 316L SS substrates. The homogeneous fine porous morphology of the pure β-TCP coating is shown in Fig. 4a and the cross-sectional view of the pure β-TCP coating on 316L SS is seen in Fig. 4b. The coating thickness of pure β-TCP is estimated as 136 μm. The EDAX pattern in Fig. 4c confirms the presence of Ca (15.18 wt%) and P (13.53 wt%) and also the presence of oxygen, which suggested the possibility of oxidation during the reaction. Fig. 4d shows the spherical morphology of 2Si-β-TCP with a homogeneous coating without any major cracks. From the cross-sectional view (Fig. 4e) the coating thickness of the 2Si-β-TCP is measured as 142 μm. The EDAX analysis of the 2Si-β-TCP coatings (Fig. 4f) shows the weight percentages of Ca, P, Si and O as 30.51, 17.99, 1.23 and 50.27

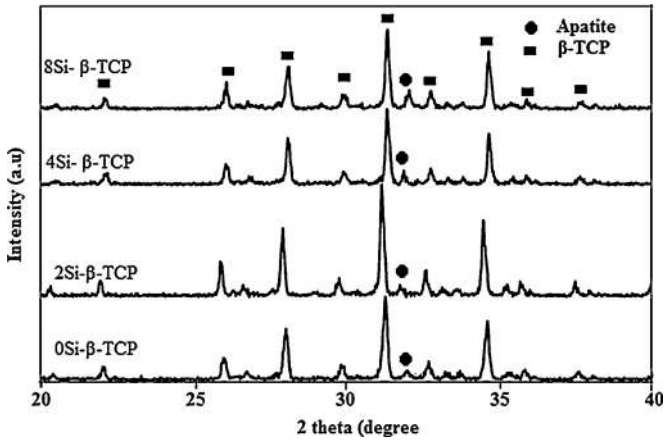

Fig. 6. The XRD pattern 0Si-β-TCP, 2Si-β-TCP, 4Si-β-TCP, and 8Si-β-TCP coated 316L SS substrate soaked in SBF solution for 28 days of incubation.

respectively. As the Si content is increased, a gradual decrease is seen in the number of large grains and an increase in the number of small grains for 4Si-β-TCP (Fig. 4g). The coating thickness is estimated as 275 μm using the cross-sectional image shown in Fig. 4h. The EDAX spectrum (Fig. 4i) for 4Si-β-TCP also confirms the presence of Ca (38.81 wt%), P (24.37 wt%), Si (5.65 wt%) and O (31.17 wt%). Fig. 4j shows the spherical morphology of the 8Si-β-TCP coating, which has a thickness of 288 μm as measured from the cross-sectional (Fig. 4k) view. The presence of Ca (40.28 wt%), P (26.34 wt%), Si (8.32 wt%) and O (33.14 wt%) in 8Si-β-TCP is confirmed from the EDAX spectrum (Fig. 4l).

3.5. SBF immersion studies

To determine the biomineralization ability of the samples, pure β-TCP, 2Si-β-TCP, 4Si-β-TCP, and 8Si-β-TCP coated 316L SS substrates were soaked in SBF solution for 7, 14, 21 and 28 days of incubation and the corresponding FESEM micrographs are shown in Fig. 5a–p. It can be clearly seen that, after soaking in SBF for 7 days, the pure β-TCP and all Si-β-TCP coated 316L SS are partially covered with a new apatite, consisting of heterogeneous particles with different shapes and sizes. After soaking for 14 days, the number of apatite layers are rapidly increased and dispersed. For 21 days of soaking time, the spherical morphology aggregates and covers the whole surface indicating the important role played by the surface chemistry. After 28 days of soaking time, the whole surface is fully covered by the apatite layer. When compared to other silica doping, the formation apatite increases for all days on 8Si-β-TCP coating. Ca ions in the SBF solution are initially attracted to the interface between the coating and solution and the Si—OH groups in the hydrated Si-β-TCP provide heterogeneous nucleation sites for apatite deposition. Fig. 6 shows the XRD peaks of pure β-TCP, 2Si-β-TCP, 4Si-β-TCP, and 8Si-β-TCP coated 316L SS substrate that are soaked in SBF solution for 28 days of incubation. The low peak intensity coupled with a peak broadening of the apatite layer is observed in all XRD patterns. This confirms the formation apatite on the surface corresponding to standard JCPDS card no. (09-0169). The apatite peak intensity increases for 8Si-β-TCP coated 316L SS confirming more biomineralization nature of this coating.

3.6. XRF analysis

The XRF data in Table 2 reveal a systematic increase in the concentration of Si with increasing molar ratios of Si, with refined values of 0.069, 0.115, 0.417 and 0.835 for 2Si-β-TCP, 4Si-β-TCP, 5Si-β-TCP, and 8Si-β-TCP respectively. This indicates the incorporation of silicon in the crystal structure. The presence of Ca, P and Si in the pure β-TCP and Si-β-TCP is determined by X-ray fluorescence. Fig. 7 shows the XRF graph of Ca/P ratio with respect to the Si-β-TCP. The Ca/P ratio of the pure β-TCP and Si-β-TCP coatings is slightly lower than the theoretical value of 1.5. The Ca/(P + Si) molar ratio is found to decrease with the increase in Si doping. This may be due to the formation of amorphous calcium phosphate and the incorporation of lower ionic radii of Si sites in the β-TCP structure.

Table 2
Chemical analysis (X-ray fluorescence) of Si-β-TCP.

Sample	Experimental composition				
	CaO (wt%)	P_2O_5 (wt%)	SiO_2 (wt%)	Ca/P	Ca/(P + Si)
0Si-β-TCP	59.230	40.67	–	1.456	–
2Si-β-TCP	59.080	40.760	0.069	1.449	1.447
4Si-β-TCP	58.820	40.930	0.115	1.437	1.433
5Si-β-TCP	58.310	41.160	0.417	1.422	1.402
8Si-β-TCP	58.160	40.900	0.835	1.416	1.393

3.7. Effects of Si additions

Silica is known to be an essential mineral element for metabolic role connected to bone growth [27]. β-TCP induces the enhanced bone growth and chemico-physical modifications such as superficial chemistry, topography and microstructure [28]. Silica generates defects in the calcium phosphate crystalline phases due to substitution of P^{5+} with Si^{4+} and also due to charge compensation mechanisms for Si substitution. Since OH does not exist in this compound, charge compensation for Si^{4+} that replaces P^{5+} in the TCP lattice requires either the formation of oxygen O^{2-} vacancies or the presence of excess calcium Ca^{2+} [29]. TCP can exist on a number of crystallographic forms, with the alpha (α-TCP) and beta (β-TCP) polymorphs, which correspond to high- and low-temperature phases respectively [30]. β-TCP is more soluble and biodegradable than HAp and it is expected that Si ions occupy P sites in the TCP network and are more labile than HAp network. Moreover, as the Si content is increased, there is a corresponding decrease in the dissolution rate that enhances the mechanical strength [31,32]. Hence, the Si-β-TCP examined in this work is a strong candidate for implant applications with improved bioactivities.

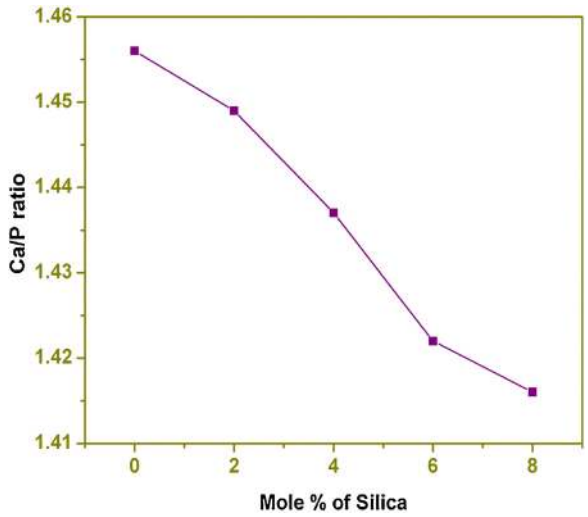

Fig. 7. XRF graph of Ca/P ratio with respect to the Si-β-TCP.

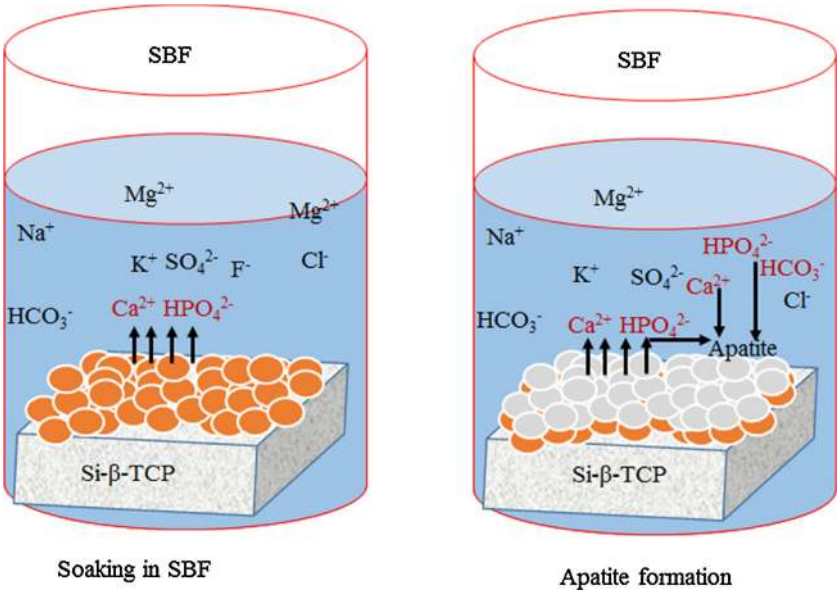

Fig. 8. The mechanism of the apatite formation on the Si-β-TCP coated 316L SS substrate in SBF solution.

3.8. Mechanism of apatite growth

Fig. 8 shows the schematic diagram of the apatite formation mechanism. When a bioceramic-coated 316L SS substrate is immersed in SBF solution, the sphere like apatite layers is formed on the surface. The presence of dense apatite layers can enhance the osteointegration and osteoconduction properties [33]. For the high ion concentration of HPO_4^{2-}, the released Ca^{2+} ions react with the HPO_4^{2-} ions, and re-precipitated as apatite. It is well known that apatite structure consists of Ca^{2+}, PO_4^{3-} and OH^- groups, which are closely packed together. The process of apatite formation depends on the large number of negative ions (i.e. PO_4^{3-} and OH^-) on the surface [34]. During incubation period, the positive Ca^{2+} ions from SBF are attracted by the OH^- and PO_4^{3-} ions present on apatite surface. Hence the increased positive charge on the surface attracts more negatively charged hydroxyl (OH^-) and phosphate (PO_4^{3-}) ions from the SBF solution [35]. Most notably, the Si—OH functional group of Si-based β-TCP has been proven to act as the nucleation center for apatite formation. This in turn increases the ionic activity product of the apatite in the surrounding fluid [36]. Also the high ion concentration of HPO_4^{2-} and the released Ca^{2+} ions react with HPO_4^{2-} ions and re-precipitated as apatite.

4. Conclusion

Pure β-TCP and Si-β-TCP coatings on 316L SS substrates are achieved using electrophoretic deposition technique. The structural, functional, morphological and chemical compositions of the coated substrates are characterized using XRD, FTIR, and SEM–EDX, FESEM and XRF analysis. The XRD results show that the incorporation of Si into the β-TCP lattice had no direct effect on its crystallographic structure with the exception of some intensity changes, which is due to the partial incorporation of Si into β-TCP structure. FTIR confirms the presence of —OH, PO_4^{3-}, and ($P_2O_7^{4-}$) functional groups. Homogeneous spherical morphology is obtained for pure β-TCP and Si-β-TCP coatings. Furthermore, the biomineralization ability of the samples is evaluated in SBF solution. The Si-β-TCP displays superior biomineralization activity with increasing silicon content. Hence the studies convey that increased silica doping supports the growth of apatite and these materials are suitable for load bearing implant application.

Conflicts of interest

The authors declare no conflicts of interest.

Acknowledgement

One of the authors, Sujin P. Jose, acknowledges University Grants Commission (UGC), New Delhi for the Indo-US Raman Fellowship.

Appendix A. Supplementary data

Supplementary data associated with this article can be found, in the online version, at doi:10.1016/j.jascer.2015.06.004

References

[1] H.F. Borhane, G. Olivier, W. Pierre, C. Daniel and L. Pierre, Biomaterials, 29, 1177–1188 (2008).
[2] E. Meurice, A. Leriche, J.C. Hornez, F. Bouchart, E. Rguiti, L. Boilet, M. Descampsa and F. Cambier, J. Eur. Ceram. Soc., 32, 2673–2678 (2012).
[3] A.M. Pietak, J.W. Reid, M.J. Stott and M. Sayer, Biomaterials, 28, 4023–4032 (2007).
[4] M. Epple, K. Ganesan, R. Heumann, J. Klesing, A. Kovtun, S. Neumann and V. Sokolova, J. Mater. Chem., 20, 18–23 (2010).
[5] S.V. Dorozhkin, J. Am. Ceram. Soc., 90, 244–249 (2007).
[6] A. Rawal, X. Wei, M. Akinc and K. Schmidt-Rohr, Chem. Mater., 20, 2583–2591 (2008).
[7] H.S. Ryu, H.J. Youn, K.S. Hong, B.S. Chang, C.K. Lee and S.S. Chung, Biomaterials, 23, 909–914 (2002).
[8] D. Choi and N.P. Kumta, Mater. Sci. Eng. C, 27, 377–381 (2007).
[9] K. Prabakaran and S. Rajeswari, Trends Biomater. Artif. Organs, 20, 20–23 (2006).
[10] K. Lin, J. Chang, J. Lu, W. Wu and Y. Zengs, Ceram. Int., 33, 979–985 (2007).
[11] B. Mirhadi, B. Mehdikhani and N. Askari, Process. Appl. Ceram., 5, 193–198 (2011).
[12] S. Ming-You, D. Shinn-Jyh and C. Hsien-Chang, Acta Biomater., 7, 2604–2614 (2011).
[13] W. Waked and J. Grauer, Orthopedics, 31, 591–597 (2008).
[14] M. Bohner, Biomaterials, 30, 6403–6406 (2009).
[15] E. Gyorgy, S. Grigorescu, G. Socol, I.N. Mihailescu, D. Janackovic, A. Dindune, Z. Kanepe, E. Palcevskis, E.L. Zdrentu and S.M. Petrescu, Appl. Surf. Sci., 253, 7981–7986 (2007).
[16] A.L. Oliveira, R.L. Reis and P. Li, J. Biomed. Mater. Res. B: Appl. Biomater., 83, 258–265 (2007).
[17] P. Ducheyne, S. Radin, M. Heughebaert and J.C. Heughebaert, Biomaterials, 11, 244–254 (1990).
[18] M. Manso, C. Jimenez, C. Morant, P. Herrero and J.M. Martinez-Duart, Biomaterials, 21, 1755–1764 (2000).

[19] I. Pereiro, C. Rodriguez-Valencia, C. Serra, E.L. Solla, J. Serra and P. Gonzalez, Appl. Surf. Sci., 258, 9192–9197 (2012).
[20] D. Gopi, V. Collins Arun Prakash, L. Kavitha, S. Kannan, P.R. Bhalaji, E. Shinyjoy and J.M.F. Ferreira, Corros. Sci., 53, 2328–2334 (2011).
[21] K. Prem Ananth, S. Suganya, D. Mangalaraj, J.M.F. Ferreira and A. Balamurugan, Mater. Sci. Eng. C, 33, 4160–4166 (2013).
[22] J. Andersson, E. Johannessen, S. Areva, N. Baccile, T. Azaıs and M. Linden, J. Mater. Chem., 17, 463–468 (2007).
[23] T. Kokubo and T. Takanawa, Biomaterials, 27, 2907–2915 (2006).
[24] B. Jong-Shing, L. Sz-Chian and C. San-Yuan, Biomaterials, 2, 53155–53161 (2004).
[25] Y. Xilin, C. Lazaro, M.J. Stott and M. Sayer, Biomaterials, 23, 4155–4163 (2002).
[26] M. Mariana, C. Raul García and C.Z. Cecília Amélia, Mater. Res., 15, 568–572 (2012).
[27] E. Boanini, M. Gazzano and A. Bigi, Acta Biomater., 6, 1882–1894 (2010).
[28] M. Sayer, A.D. Stratilatov, J. Reid, L. Calderin, M.J. Stott, X. Yin, M. Mackenzie, T.J.N. Smith, J.A. Hendry and S.D. Langstaff, Biomaterials, 24, 369–382 (2002).
[29] A. Pietak, J.W. Reid and M. Sayer, Biomaterials, 24, 3819–3830 (2005).
[30] M. Yashima and A. Sakai, Chem. Phys. Lett., 372, 779–783 (2003).
[31] S. Ni, K.J. Lin, J. Chang and L. Chou, J. Biomed. Mater. Res. Part A, 85, 72–82 (2008).
[32] C.X. Wang, X. Zhou and M. Wang, Mater. Charact., 52, 301–307 (2004).
[33] F.H. Jones, Surf. Sci. Rep., 42, 175–205 (2001).
[34] N.C. Pradnya, M.B. Manjushri, U.M. Ravindra, P.M. Megha and S.K. Rajendra, Mater. Sci. Eng. B, 168, 224–230 (2010).
[35] S. Prakash Parthiban, R.V. Sugandhi, E.K. Girija, K. Elayaraja, P.K. Kulriya, Y.S. Katharria, F. Singh, I. Sulania, A. Tripathi, K. Asokan, D. Kanjilal, S. Yadav, T.P. Singh, Y. Yokogawa and S. Narayana Kalkura, Nucl. Instrum. Methods Phys. Res. B, 266, 911–917 (2008).
[36] S.J. Ding, M.Y. Shie and C.Y. Wang, J. Mater. Chem., 19, 1183–1190 (2009).